The Journal of Experimental Biology 215, 1106-1116

doi:10.1242/jeb.062273

RESEARCH ARTICLE

Proteomic responses of blue mussel (*Mytilus*) congeners to temperature acclimation

Peter A. Fields[1,*], Marcus J. Zuzow[2] and Lars Tomanek[2]

[1]Franklin & Marshall College, Biology Department, PO Box 3003, Lancaster, PA 17604-3003, USA and [2]California Polytechnic State University, Department of Biological Sciences, Center for Coastal Marine Sciences, Environmental Proteomics Laboratory, 1 Grand Avenue, San Luis Obispo, CA 93407-0401, USA

*Author for correspondence (peter.fields@fandm.edu)

Accepted 6 December 2011

SUMMARY

The ability to acclimate to variable environmental conditions affects the biogeographic range of species, their success at colonizing new habitats, and their likelihood of surviving rapid anthropogenic climate change. Here we compared responses to temperature acclimation (4 weeks at 7, 13 and 19°C) in gill tissue of the warm-adapted intertidal blue mussel *Mytilus galloprovincialis*, an invasive species in the northeastern Pacific, and the cold-adapted *M. trossulus*, the native congener in the region, to better understand the physiological differences underlying the ongoing competition. Using two-dimensional gel electrophoresis and tandem mass spectrometry, we showed that warm acclimation caused changes in cytoskeletal composition and proteins of energy metabolism in both species, consistent with increasing rates of filtration and respiration due to increased ciliary activity. During cold acclimation, changes in cytoskeletal proteins were accompanied by increasing abundances of oxidative stress proteins and molecular chaperones, possibly because of the increased production of aldehydes as indicated by the upregulation of aldehyde dehydrogenase. The cold-adapted *M. trossulus* showed increased abundances of molecular chaperones at 19°C, but *M. galloprovincialis* did not, suggesting that the two species differ in their long-term upper thermal limits. In contrast, the warm-adapted *M. galloprovincialis* showed a stronger response to cold acclimation than *M. trossulus*, including changes in abundance in more proteins and differing protein expression profiles between 7 and 13°C, a pattern absent in *M. trossulus*. In general, increasing levels of oxidative stress proteins inversely correlate with modifications in Krebs cycle and electron transport chain proteins, indicating a trade-off between oxidative stress resistance and energy production. Overall, our results help explain why *M. galloprovincialis* has replaced *M. trossulus* in southern California over the last century, but also suggest that *M. trossulus* may maintain a competitive advantage at colder temperatures. Anthropogenic global warming may reinforce the advantage *M. galloprovincialis* has over *M. trossulus* in the warmer parts of the latter's historical range.

Supplementary material available online at http://jeb.biologists.org/cgi/content/full/215/7/1106/DC1

Key words: acclimation, biogeography, climate change, cold stress, heat stress, *Mytilus galloprovincialis*, *Mytilus trossulus*, proteomics, systems biology, temperature.

INTRODUCTION

Temperature strongly affects rates of physiological processes and the integrity of macromolecular structures in cells, and thus plays an important role in limiting the range species can occupy (Hochachka and Somero, 2002; Pörtner, 2010; Tomanek, 2008; Tomanek, 2010). Increasing average global surface temperatures over the last three decades (0.6°C) (Hansen et al., 2006) correlate with a number of recently documented range shifts that are generally consistent with a temperature-driven range expansion of warm-adapted and range contraction of cold-adapted species at temperate northern latitudes, in both terrestrial (Parmesan et al., 1999; Thomas and Lennon, 1999) and marine (Barry et al., 1995; Mieszkowska et al., 2006) habitats. In order to predict which organisms will be affected most by anthropogenic temperature increases, we need to better understand the mechanisms by which temperature affects the physiology of organisms and, specifically, identify the cellular processes that are most sensitive to acute and chronic heat stress.

To address these questions, comparisons of closely related species (e.g. congeners) that differ in thermal tolerance and show recent range shifts may be especially useful. For example, the mussel genus *Mytilus* has been examined by a number of researchers, with several studies documenting recent range shifts by *M. edulis* along the Atlantic coast of North America (Jones et al., 2009), and by *M. trossulus* and *M. galloprovincialis* along the Pacific coast of North America (Sarver and Foltz, 1993; Wonham, 2004; Hilbish et al., 2010). Although these range shifts are likely to be affected by a number of biotic and abiotic factors, e.g. salinity (Braby and Somero, 2006a; Jones et al., 2009; Schneider, 2008), the above studies indicate that temperature is a crucial feature setting latitudinal range boundaries for each of the *Mytilus* species.

The *M. trossulus–M. galloprovincialis* species pair is especially informative because these congeners are closely related and the latter is an invasive species in the eastern Pacific, which is replacing the former throughout much of its original range in what appears to be a temperature-dependent fashion. *Mytilus galloprovincialis*, native to the Mediterranean, is thought to have first invaded southern California at the beginning of the last century (Geller, 1999). Since then it has displaced the native *M. trossulus* in the southern portion of its historical range, from Baja California north to central California, where a hybrid zone marks the current southern limit of *M. trossulus*. Single-species populations of *M. trossulus* are found north of the hybrid region into the Arctic, although isolated populations of *M. galloprovincialis* occur

in Washington, perhaps as a result of independent invasion events. These differences in ranges, combined with studies examining the physiological (Schneider, 2008; Braby and Somero, 2006) and biochemical (Hofmann and Somero, 1996; Fields et al., 2006) responses of these congeners to increasing temperature, suggest that *M. galloprovincialis* is better able to compete in warmer conditions whereas *M. trossulus* is being restricted to regions with cooler temperatures.

Researchers have used congeners of the blue mussel complex to investigate changes in proteins in response to chronic temperature stress and have shown acclimation- and acclimatization-induced shifts in the synthesis of heat shock proteins (Hsps) (Hofmann and Somero, 1996) and pyruvate kinase, and the phosphorylation of stress-activated protein kinases (Anestis et al., 2007; Ioannou et al., 2009; Evans and Somero, 2010). However, to more fully describe the physiological differences between these *Mytilus* congeners that may provide *M. galloprovincialis* a competitive advantage over *M. trossulus* in warmer habitats, recent studies have taken a systems biology approach. For example, complementary studies of the transcriptomic (Lockwood et al., 2010) and proteomic (Tomanek and Zuzow, 2010) responses of both species to acute heat stress have provided a more comprehensive understanding of cellular responses to heat stress generally, as well as the differences in response between these two congeners.

Although proteomics studies generally are limited to the detection of medium- to high-abundance and mostly hydrophilic proteins (Lovrić, 2010), recent comparative proteomics studies have generated a number of new hypotheses about how organisms respond to environmental stress, for example, how post-translational modifications may regulate the cellular response to oxidative stress (for reviews, see Sheehan, 2007; Tomanek, 2011). Proteomics studies on mollusks in particular have characterized the response to oxidative stress and pollutant exposure (Apraiz et al., 2006; McDonagh and Sheehan, 2007) as well as hypercapnia (Tomanek et al., 2011). Here we employ a proteomic analysis to better understand cellular responses to chronic temperature stress, because the acute diurnal fluctuations in temperature the *Mytilus* congeners experience are overlaid on a seasonal pattern of temperature variation. As anthropogenic global warming increases in rate and magnitude, intertidal organisms such as *Mytilus* will need to cope with stresses on multiple time scales, and changes in habitat temperature may alter the competitive balance between the native and the invasive species. The present study characterizes the proteomic response of *M. trossulus* and *M. galloprovincialis* to chronic temperature acclimation during constant immersion in the laboratory. We use two-dimensional (2-D) gel electrophoresis to separate proteins purified from gill tissue of temperature-acclimated *M. trossulus* and *M. galloprovincialis* individuals, and identify *via* mass spectrometry those proteins that change in abundance after acclimation.

MATERIALS AND METHODS

Animal collection, maintenance and experimental design

Mytilus trossulus Gould 1850 and *M. galloprovincialis* Lamarck 1819 were collected subtidally from Newport, OR, USA (44°38′25″N, 124°03′10″W) and Santa Barbara, CA, USA (34°24′15″N, 119°41′30″W), respectively. In a separate study, PCR was used to confirm that each site was occupied by only a single species (i.e. there were no hybrids present) (Lockwood et al., 2010). Animals were kept for 4 weeks under constant immersion at 7, 13 or 19°C in recirculating seawater tanks and fed a phytoplankton diet every day. Following acclimation, gill tissue of both congeners was collected and immediately frozen using liquid nitrogen (N=6 per species for each treatment). Tissues were subsequently kept at –80°C until homogenization.

Homogenization

Sample preparation followed procedures outlined previously (Tomanek and Zuzow, 2010). Briefly, gill tissue was lysed in homogenization buffer [7 mol l^{-1} urea, 2 mol l^{-1} thiourea, 1% amidosulfobetaine (ASB)-14, 40 mmol l^{-1} Tris-base, 0.5% immobilized pH 4–7 gradient (IPG) buffer (GE Healthcare, Piscataway, NJ, USA) and 40 mmol l^{-1} dithiothreitol] at a ratio of 1:4. After centrifugation at 20°C for 30 min at 16,100 ***g***, the proteins were precipitated by adding four volumes of ice-cold 10% trichloroacetic acid in acetone and incubating the solution at –20°C overnight. The precipitate was centrifuged at 4°C for 15 min at 18,000 ***g***, the supernatant was discarded and the protein pellet was washed with ice-cold acetone and centrifuged again at 4°C. After air-drying, the pellet was re-suspended in rehydration buffer [7 mol l^{-1} urea, 2 mol l^{-1} thiourea, 2% cholamidopropyl-dimethylammonio-propanesulfonic acid (CHAPS), 2% nonyl phenoxylpolyethoxylethanol (NP)-40, 0.002% Bromophenol Blue, 0.5% IPG buffer and 100 mmol l^{-1} dithioerythritol] through repeated vortexing. The protein concentration was determined with the 2-D Quant kit (GE Healthcare), according to the manufacturer's instructions.

2-D gel electrophoresis

Proteins were separated by isoelectric point using IPG strips (pH 4–7, 11 cm; GE Healthcare). Samples were diluted to 2 μg μl^{-1} with rehydration buffer, and 200 μl was loaded onto each strip in one well of an isoelectric focusing cell (BioRad, Hercules, CA, USA) *via* 5 h of passive rehydration, followed by 12 h of active rehydration (50 V). Separation and focusing was accomplished by exposing strips to 500 V for 1 h, 1000 V for 1 h and 8000 V for 2.5 h (all voltage changes occurred in rapid mode; maximum current 50 μA). Following focusing, strips were frozen at –80°C.

To prepare for 2nd dimension SDS-PAGE electrophoresis, strips were incubated in equilibration buffer (375 mmol l^{-1} Tris-base, 6 mol l^{-1} urea, 30% glycerol, 2% SDS and 0.002% Bromophenol Blue) for two 15 min intervals, first with 65 mmol l^{-1} dithiothreitol and second with 135 mmol l^{-1} iodoacetamide. IPG strips then were placed on top of 11.8% polyacrylamide gels, which were run (Criterion Dodeca; BioRad) at 200 V for 55 min at 10°C. Gels were subsequently stained with colloidal Coomassie Blue (G-250) overnight and destained by washing repeatedly with Milli-Q water for 48 h. The resulting gel images were scanned with an Epson 1280 transparency scanner (Epson, Long Beach, CA, USA).

Gel image analysis

Digitized images of 2-D gels were analyzed using Delta2D (version 3.6; Decodon, Greifswald, Germany) (Berth et al., 2007). Spots were detected on gels by fusing all images from one species into a composite image (Fig. 1). Spot boundaries were detected on this composite image and transferred back to the original gel images. After background subtraction, the relative amount of protein in each spot (i.e. spot volume) was quantified by normalizing against total spot volume of all proteins in the gel image.

To determine which proteins changed in volume significantly in response to acclimation temperature, we used a one-way ANOVA (P<0.02) within each species and with temperature as the main effect. We generated a null distribution for the one-way ANOVA (1000 permutations) to account for the unequal variance and non-normal distributions of the response variables. We chose a P-value

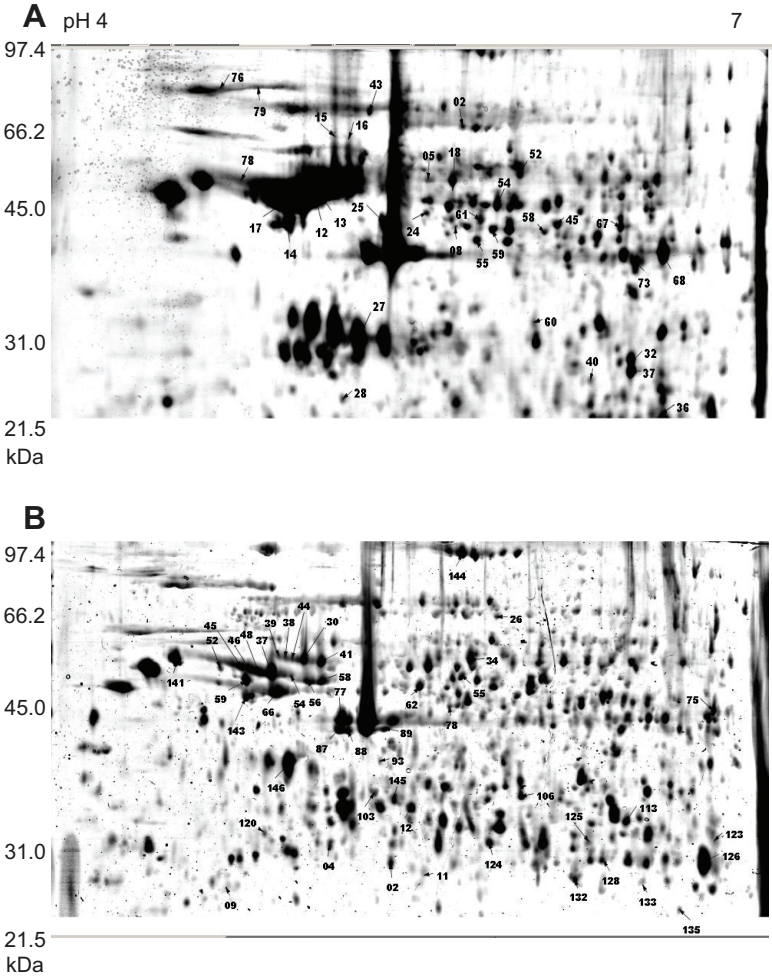

Fig. 1. Protein samples from (A) *Mytilus trossulus* and (B) *M. galloprovincialis* gill tissue after acclimation to 7, 13 and 19°C, separated by isoelectric point (horizontal axis) and mass (vertical axis) on two-dimensional gels. Each panel represents a composite gel image (or proteome map) of all 18 gels (N=6 per treatment; three treatments per species) depicting 331 and 458 protein spots from gill tissue of each species, respectively. The proteome maps represent average pixel volumes for each protein spot. Numbered spots were those that showed changes in abundance in response to chronic temperature acclimation (one-way ANOVA, P<0.02) and were identified using tandem mass spectrometry (for protein identifications see Figs 2, 3, and supplementary material Tables S1, S2).

of 0.02 to limit the number of false positives instead of using a multiple-comparison correction. Because there is only limited overlap between the proteome maps of the two congeners, as well as uncertainty whether overlapping proteins were orthologous or paralogous homologs, a two-way ANOVA comparing species was not possible. Following the one-way ANOVA, *post hoc* testing to compare treatments was conducted using Tukey's analysis (P<0.05), using MiniTab (version 15; Minitab Inc., State College, PA, USA), to support conclusions about differences in single protein expression profiles (single-protein graphs are not shown).

Mass spectrometry

Proteins that changed in abundance in response to temperature acclimation were excised from gels. Gel plugs were destained twice with 25 mmol l^{-1} ammonium bicarbonate in 50% acetonitrile, dehydrated with 100% acetonitrile and digested with 11 ng μl^{-1} trypsin (Promega, Madison, WI, USA) overnight at 37°C. Digested proteins were extracted using elution buffer [0.1% trifluoroacetic acid (TFA)/acetonitrile; 2:1] and concentrated using a SpeedVac centrifugal concentrator (Thermo Fisher Scientific, Waltham, MA, USA). The elution buffer containing the digested protein was mixed with 5 µl of matrix solution (0.2 mg ml^{-1} α-hydroxycyano cinnamic acid in acetonitrile) and spotted on an Anchorchip^{TM} target plate (Bruker Daltonics Inc., Billerica, MA, USA). The spotted proteins were washed with 0.1% TFA and recrystallized using an acetone/ethanol/0.1% TFA (6:3:1) mixture.

We obtained peptide mass fingerprints (PMFs) using a matrix-assisted laser desorption ionization tandem time-of-flight (MALDI-TOF-TOF) mass spectrometer (Ultraflex II; Bruker Daltonics Inc.). We selected a minimum of six peptides for tandem mass spectrometry in order to obtain information about the b- and y-ions of the peptide sequence for use in subsequent protein identification. Analysis of peptide spectra followed previously published procedures (Tomanek and Zuzow, 2010). We used flexAnalysis (version 3.0; Bruker Daltonics Inc.) to detect peptide peaks (SNAP algorithm with a signal-to-noise ratio of 6 for MS and 1.5 for MS/MS). Porcine trypsin was used for internal mass calibration.

To identify proteins we used Mascot (version 2.2; Matrix Science Inc., Boston, MA, USA) and combined PMFs and tandem mass spectra in a search against two databases. One database is an EST library that initially contained approximately 26,000 entries, representing 12,961 and 1688 different gene sequences for *M. californianus* and *M. galloprovincialis*, respectively (Lockwood et al., 2010). The other was Swiss-Prot (June 2009), with 17,360 molluscan protein sequences. Oxidation of methionine and carbamidomethylation of cysteine were our only variable modifications. Our search allowed one missed cleavage during trypsin digestion. For tandem mass spectrometry we set the precursor-ion mass tolerance to 0.6 Da, the default value in Mascot. The molecular weight search (MOWSE) score that indicated a significant hit was dependent on the database: scores higher than 40 and 51 were significant (P<0.05) for a search in the *Mytilus* EST

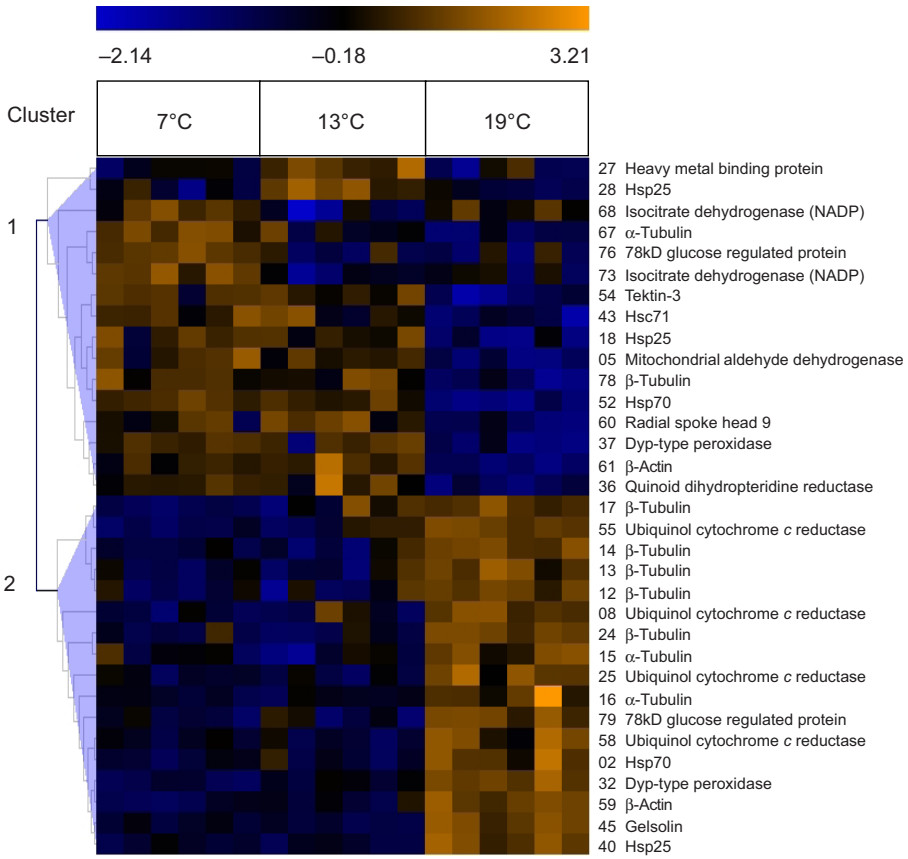

Fig. 2. Hierarchal clustering using Pearson's correlation of *Mytilus trossulus* protein spots that changed significantly with temperature acclimation, identified with tandem mass spectrometry. Blue coloring represents a lower than average protein abundance (standardized values using normalized volumes), whereas orange represents greater than average protein abundance. The columns show individual mussels, which cluster according to treatment (N=6 for each treatment). The rows represent the standardized expression patterns of proteins, which are identified to the right. Clustering reveals two major groups of proteins with similar expression patterns.

and Swiss-Prot databases, respectively. However, we only accepted positive identifications that included two matched peptides regardless of the MOWSE score.

Statistical analysis

To associate proteins with similar expression patterns across samples, and to group mussels with similar protein expression profiles, we employed hierarchical clustering with average linking (Delta2D) using a Pearson correlation metric. To further assess the importance of specific proteins in differentiating the proteomes of mussels acclimated to different temperatures, we also employed principal component analyses (PCAs; Delta2D); these PCAs were based on proteins whose expression profiles changed significantly after acclimation and that were identified with mass spectrometry (ANOVA, P<0.02). (PCAs were also performed for each species using all spots detected, and the separation of acclimation groups in each of these PCAs was not qualitatively different from that in PCAs that included only identified spots.) Component loadings, which quantify the contribution of each protein to the separation of samples along a given component, were used to compare changes in protein expression both among temperatures and between species.

RESULTS

Changes in protein abundance

The results described below are based on changes in protein abundance in gill of *M. trossulus* and *M. galloprovincialis* after acclimation to different temperatures. It is important to note that protein abundance can change because of synthesis, post-translational modifications (PTMs) or degradation. Thus, when we refer to abundance changes of protein spots or changes in protein expression, one or a combination of these processes may be responsible.

2-D gel image analysis

Following acclimation of mussels to constant immersion at 7, 13 and 19°C, we separated protein samples from gill tissue of both species *via* 2-D gel electrophoresis (2DGE) (Fig. 1). We detected 331 and 458 protein spots from *M. trossulus* and *M. galloprovincialis*, respectively. Of these, 23.9% (79 spots) changed in abundance among *M. trossulus* acclimated to different temperatures, of which 33 spots were identified *via* MS/MS (supplementary material Table S1). In comparison, 32.8% (150 spots) changed in *M. galloprovincialis* in response to temperature acclimation, of which we identified 48 (supplementary material Table S2).

Hierarchical clustering of protein expression patterns

Fig. 2 shows the hierarchical clustering of *M. trossulus* samples (i.e. individual mussels, arrayed in columns) and of identified protein isoforms (arrayed in rows) that significantly (ANOVA, P<0.02) differ in abundance following temperature acclimation. Fig. 3 shows the comparable hierarchical clustering of samples and proteins from *M. galloprovincialis*. For each species, samples cluster clearly by acclimation temperature, indicating that acclimation to each of the three temperatures significantly altered protein expression profiles.

Examination of Figs 2 and 3 reveals that whereas *M. trossulus* acclimated to 7 and 13°C have roughly comparable protein expression patterns, i.e. there are only two major protein clusters that differentiate 7 and 13°C together from 19°C (clusters 1–2; Fig. 2), *M. galloprovincialis* proteins cluster in four major groups (clusters 1–4; Fig. 3), with the 7, 13 and 19°C acclimated groups having distinct expression profiles.

Clusters 1 and 2 are comparable between the two species: cluster 1 includes proteins upregulated at 7 and 13°C but downregulated at 19°C; cluster 2 includes proteins with the reverse pattern. The latter cluster is characterized in both species by the upregulation at

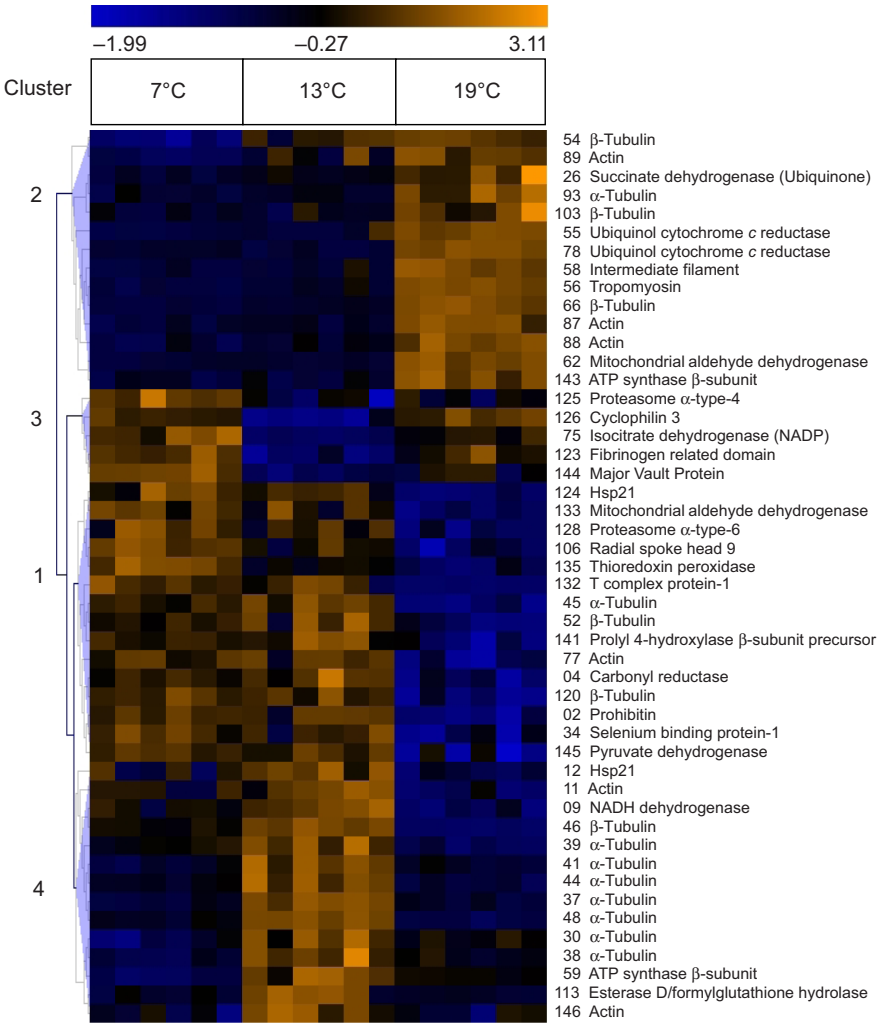

Fig. 3. Hierarchal clustering using Pearson's correlation of *Mytilus galloprovincialis* protein spots that changed significantly with temperature acclimation, identified with tandem mass spectrometry. The clustering shows four major groups of proteins with similar expression patterns. For further details see Fig. 2.

19°C of cytoskeletal proteins, e.g. actin and tubulin, as well as energy-generating proteins of the electron transport chain (ETC), e.g. ubiquinol cytochrome *c* reductase. In the case of *M. trossulus*, the relatively cold-adapted congener, this cluster also includes the upregulation at 19°C of molecular chaperones, e.g. Hsp25, Hsp70 and glucose-regulated protein 78 (Grp78), and one oxidative stress protein, Dyp-type peroxidase. However, in *M. trossulus*, each of these proteins has two or more isoforms, one that is upregulated at 19°C and at least one other that is upregulated at 7 and 13°C (Fig. 2). Inversely correlated changes in abundance of isoforms of the same protein may be due to differing PTMs or combinations of PTMs (Walsh et al., 2005) that alter the positions of the protein on the 2-D gel, and this is our interpretation of the changing abundance of Hsps in *M. trossulus* after temperature acclimation. However, we cannot determine from abundance data whether a particular shift in position on the 2-D gel, due to a specific PTM, leads to an increase or decrease in chaperoning activity. One Hsp25 isoform in *M. trossulus* (spot 18) is notable because its molecular mass estimated from the 2-D gel is more than double the predicted mass (supplementary material Table S1).

Cluster 1, characterized by the upregulation of proteins at 7 and 13°C, shows fewer cytoskeletal proteins but a number of chaperones (five in *M. trossulus*, and three in *M. galloprovincialis*, including cyclophilin 3, T complex protein-1 and prohibitin), proteins involved in energy metabolism, e.g. pyruvate dehydrogenase (in *M. galloprovincialis*) and isocitrate dehydrogenase (*M. trossulus*), and several oxidative stress proteins (see below for discussion), e.g. Dyp-type peroxidase (*M. trossulus*), and thioredoxin peroxidase and carbonyl reductase (*M. galloprovincialis*).

The two species are differentiated, however, by the presence of two additional protein clusters that are found only in *M. galloprovincialis* (clusters 3 and 4; Fig. 3) and that separate mussels acclimated to 7°C from those acclimated to 13°C. The presence of these clusters suggests that *M. galloprovincialis*, the relatively warm-adapted congener, is more sensitive to the difference between these lower temperatures than *M. trossulus*. Cluster 3, which includes proteins with relatively high abundance at 7 and 19°C but low abundance at 13°C, is the smallest cluster, with only five proteins. These five proteins are members of varied functional groups, including some (major vault protein, fibrinogen-like domain) whose function is unclear. Cluster 4 comprises proteins upregulated at 13°C relative to the other two treatment temperatures, and is significantly larger than cluster 3, with 14 proteins (29% of identified proteins). This cluster is dominated by cytoskeletal proteins (10 of 14), but includes two proteins associated with energy generation as well as a small Hsp.

Principal component analyses

PCAs were conducted to further assess the impact of the three acclimation temperatures on protein expression in the *Mytilus* congeners. Generally, the outcome of the PCAs supports the results described above for our hierarchical cluster analysis – both species

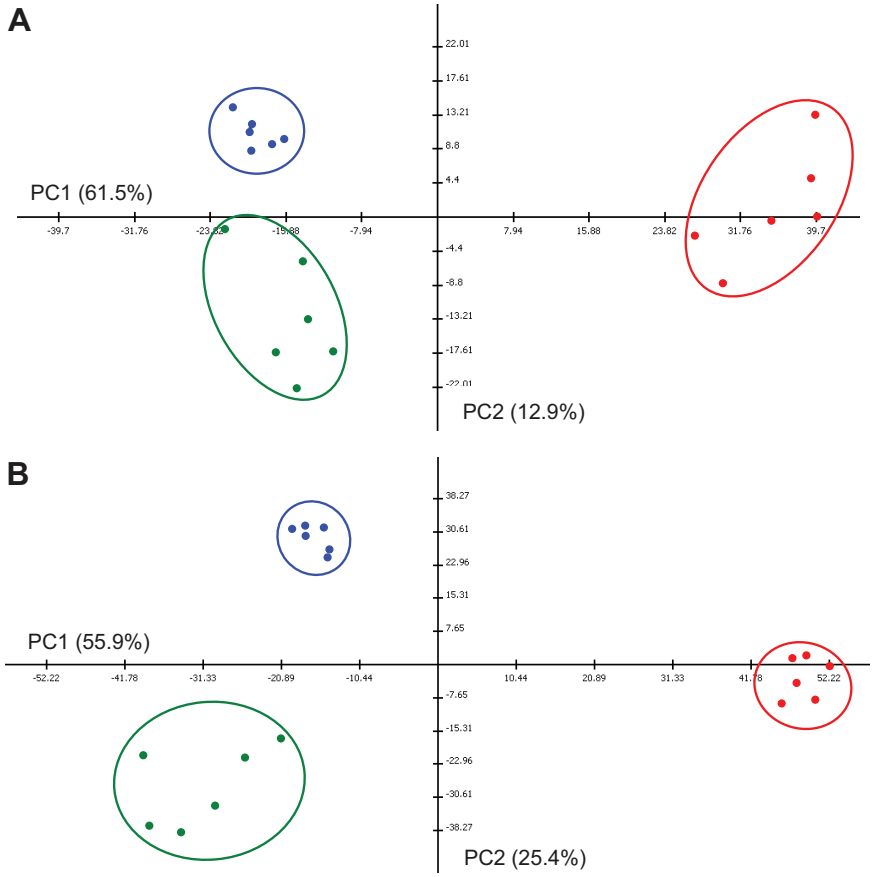

Fig. 4. Principal component analysis of temperature treatments for (A) *Mytilus trossulus* and (B) *M. galloprovincialis*, using proteins that differed significantly in abundance after acclimation to one of three treatment temperatures (one-way ANOVA, Figs 2, 3). Each symbol represents a mussel acclimated to 7°C (blue), 13°C (green) or 19°C (red). In each panel the horizontal axis represents PC1, which separates the 7°C- and 13°C-acclimated samples from the 19°C-acclimated samples in both species, and the vertical axis represents PC2, which separates the 7°C-acclimated samples from the 13°C-acclimated samples. Percentages represent the proportion of total variation in the data set described by each component.

show a significant change in protein expression pattern in response to acclimation to 19°C, but *M. galloprovincialis* is more strongly affected by the difference in temperature between the 7°C and 13°C acclimation treatments. Note that because of the variation between the proteomes of these congeners, it was not possible to overlap protein spots and assume homologies, thus we conducted a separate PCA for each species (Fig. 4).

In both species, the first component (horizontal axis) differentiates the 7°C and 13°C acclimation groups from the 19°C group; in *M. trossulus* (Fig. 4A), PC1 explains 61.5% of the variation in expression of the 33 identified proteins, whereas in *M. galloprovincialis* (Fig. 4B), PC1 explains 55.9% of the variation among the 48 identified protein spots. The second component (vertical axis) most clearly separates the 7°C and 13°C acclimation groups in both species. Notably, however, PC2 in *M. trossulus* accounts for only 12.9% of protein expression variation, but for *M. galloprovincialis* PC2 encompasses approximately double that amount, 25.4%.

The component loadings associated with these PCAs quantify the contribution of each protein to the variation explained by each PC. For example, in the case of PC1, proteins with highly positive loadings are relatively upregulated in the 19°C groups and proteins with highly negative loadings are relatively upregulated in the 7°C and 13°C groups. Among the proteins with the 10 highest positive loadings for PC1 in *M. galloprovincialis*, only proteins that are part of the cytoskeleton or are involved in energy metabolism are found (Table 1A). In contrast, in *M. trossulus*, the highest positive loadings for PC1 comprise four proteins of the cytoskeleton, including gelsolin, two molecular chaperones and three proteins involved in energy metabolism as well as one oxidative stress protein, Dyp-type peroxidase (Table 1A). Negative loadings for *M. galloprovincialis* on PC1, which indicate proteins that were upregulated at 7 and 13°C relative to 19°C, include five cytoskeletal proteins, one protein involved in energy metabolism, two molecular chaperones and one oxidative stress protein (Table 1B). The possible role of prolyl 4-hydroxylase will be discussed below. A similar pattern is seen for *M. trossulus* (Table 1B), although proteins highly upregulated after cold acclimation in this species include three putative oxidative stress proteins.

The second component most significantly separates the 7°C from the 13°C treatment group in both species (Fig. 4). Along PC2, *M. trossulus* has relatively few proteins with high loadings (either positive or negative) relative to *M. galloprovincialis* (Table 1C,D), indicative of the small variance explained by this component in the former species, and supporting the relative insensitivity of *M. trossulus* to the difference between the 7°C and 13°C acclimation treatments demonstrated by the hierarchical cluster analysis (Fig. 2).

The highest positive loadings of the second component in the more cold-sensitive *M. galloprovincialis*, which indicate upregulation at 7°C relative to 13°C, include proteins with a range of cellular functions, including cellular stress (major vault protein), oxidative stress (NADP-dependent IDH and thioredoxin peroxidase) and protein homeostasis (a proteasome subunit and cyclophilin) (Table 1C). In *M. trossulus*, two isoforms of NADP-dependent IDH and Grp78 as well as tubulin have the highest positive loadings, with other proteins contributing relatively little to the variance in PC2 (Table 1C). The 10 proteins with the highest negative loadings of PC2 for *M. galloprovincialis* are mainly isoforms of tubulin and actin, with ATP synthase and esterase D being the exceptions (Table 1D). Again, *M. trossulus* has few

Table 1. Positive and negative component loadings for PCAs shown in Fig. 4

	Mytilus trossulus		*Mytilus galloprovincialis*	
Component loading rank	Protein (spot ID)	Component loading	Protein (spot ID)	Component loading
A. Positive component loadings for PC1				
1	Gelsolin (45)	1.222	Ubiquinol cytochrome *c* reductase (78)	1.334
2	Hsp25 (40)	1.211	Mitochondrial aldehyde dehydrogenase (62)	1.312
3	Dyp-type peroxidase (32)	1.204	β-Tubulin (66)	1.296
4	β-Actin (59)	1.199	Tropomyosin (56)	1.286
5	Ubiquinol cytochrome *c* reductase (55)	1.132	Intermediate filament (58)	1.263
6	β-Tubulin (24)	1.127	Actin (87)	1.261
7	Ubiquinol cytochrome *c* reductase (25)	1.120	Actin (88)	1.256
8	β-Tubulin (14)	1.110	ATP synthase, β subunit (143)	1.248
9	78kD glucose regulated protein (79)	1.084	Ubiquinol cytochrome *c* reductase (55)	1.242
10	Ubiquinol cytochrome *c* reductase (58)	1.078	α-Tubulin (93)	1.188
B. Negative component loadings for PC1				
1	Hsp70 (52)	–1.203	α-Tubulin (45)	–1.264
2	Tektin (54)	–1.062	Prohibitin (02)	–1.232
3	Dyp-type peroxidase (37)	–1.060	β-Tubulin (120)	–1.194
4	β-Actin (61)	–1.036	Actin (77)	–1.192
5	Mitochondrial aldehyde dehydrogenase (05)	–1.025	β-Tubulin (46)	–1.191
6	β-Tubulin (78)	–1.003	Carbonyl reductase (04)	–1.154
7	Hsc71 (43)	–0.989	Prolyl 4-hydroxylase β-subunit precursor (141)	–1.122
8	Hsp25 (18)	–0.971	T-complex protein 1 (132)	–1.113
9	Quinoid dihydropteridine reductase (36)	–0.964	Pyruvate dehydrogenase (145)	–1.109
10	α-Tubulin (67)	–0.959	β-Tubulin (52)	–1.098
C. Positive component loadings for PC2				
1	Isocitrate dehydrogenase (68)	2.378	Major vault protein (144)	1.856
2	Isocitrate dehydrogenase (73)	2.352	Isocitrate dehydrogenase (75)	1.719
3	78kD glucose regulated protein (76)	2.101	Fibrinogen related domain (123)	1.677
4	α-Tubulin (67)	1.299	Proteasome α-type 4 (125)	1.499
5	α-Tubulin (15)	0.871	Thioredoxin peroxidase (135)	1.475
6	Ubiquinol cytochrome *c* reductase (58)	0.728	Cyclophilin 3 (126)	1.291
7	Gelsolin (45)	0.486	Radial spoke head 9 (106)	1.132
8	Hsp70 (52)	0.465	Proteasome α-type 4 (128)	0.852
9	β-Tubulin (24)	0.413	Mitochondrial aldehyde dehydrogenase (133)	0.734
10	78kD glucose regulated protein (76)	0.391	Hsp21 (124)	0.605
D. Negative component loadings for PC2				
1	Heavy metal binding protein (27)	–2.091	ATP synthase β-subunit (59)	–1.750
2	Hsp25 (28)	–1.964	α-Tubulin (30)	–1.737
3	β-Tubulin (17)	–1.255	α-Tubulin (38)	–1.688
4	β-Actin (61)	–0.964	α-Tubulin (41)	–1.580
5	Radial spoke head 9 (60)	–0.856	α-Tubulin (37)	–1.562
6	Ubiquinol cytochrome *c* reductase (55)	–0.523	β-Tubulin (54)	–1.525
7	β-Tubulin (12)	–0.508	α-Tubulin (44)	–1.393
8	β-Tubulin (13)	–0.429	Actin (146)	–1.381
9	Ubiquinol cytochrome *c* reductase (08)	–0.422	α-Tubulin (48)	–1.363
10	β-Actin (59)	–0.260	Esterase D/formylglutathione hydrolase (113)	–1.298

The 10 proteins with the highest positive and negative loadings are listed for both *M. trossulus* and *M. galloprovincialis*. For PC1 (A,B), positive loadings indicate proteins with relatively high abundance in samples to the right along the horizontal axis of Fig. 4 (19°C); negative loadings indicate proteins with high abundance in samples to the left (7 and 13°C). For PC2 (C,D), positive loadings indicate proteins with relatively high abundance in samples towards the top along the vertical axis of Fig. 4 (7°C); negative loadings indicate proteins with high abundance in samples towards the bottom (13°C).

proteins with high negative component loadings for PC2, with a value above 1.0 for only three proteins: a heavy metal binding protein, Hsp25 and a β-tubulin isoform (Table 1D). To reiterate, the component loadings of PC2 indicate that *M. galloprovincialis* responds strongly to the difference between 7 and 13°C, whereas *M. trossulus* does not.

DISCUSSION

Thermal range of *Mytilus* congeners

A number of studies have provided evidence that *M. galloprovincialis* is the more warm-adapted (but cold-sensitive) of the two congeners (e.g. Braby and Somero, 2006; Schneider and Helmuth, 2007). Based on seasonal seawater temperature data (Ioannou et al., 2009), 7°C is a temperature *M. galloprovincialis* may rarely experience within its native (Mediterranean) environment. It can endure long-term exposure to 28°C, however, with 70% of individuals surviving this temperature for at least 30 days under laboratory conditions (Anestis et al., 2007). In contrast, 21°C is an acclimation temperature at which *M. trossulus* experiences high levels of mortality (Braby and Somero, 2006). Further, winter-acclimatized *M. trossulus* induced Hsp synthesis after acute exposure to 23°C (Buckley et al., 2001). At lower temperatures, *M. trossulus* acclimated to 7°C had a heart rate two to three times higher than that of *M. galloprovincialis* acclimated

to the same temperature, and *M. trossulus* was able to maintain a higher heart rate when acutely exposed to lower temperatures (Braby and Somero, 2006). We can summarize, then, that 7°C appears to induce physiological stress in *M. galloprovincialis*, whereas 19°C may approach the long-term upper thermal limit of *M. trossulus*.

Comparing proteomes of closely related congeners

We know of few comparative proteomics studies examining effects of environmental stress on closely related species (Tomanek and Zuzow, 2010; Serafini et al., 2011); such studies have been uncommon in part because comparing proteomes between species poses several conceptual and technical challenges. First, even the proteomes of closely related species differ enough to prevent a simple matching of proteome maps, which limits our ability to apply a single PCA to the combined data set of both species. Second, protein abundance comparisons ideally should be between orthologous homologs with the same PTMs, which requires that the mass spectra cover a high percentage of each protein sequence to confirm close homology, as well as identify all the peptides that carry PTMs. Third, because a single amino acid change or PTM can alter the isoelectric point of a protein significantly, homologous protein isoforms between congeners may occur outside the pH range being analyzed (pH 4–7 in this study). Finally, because of the lack of a full genome sequence in *Mytilus*, it is possible that certain homologs are not included in the protein or nucleotide databases and thus cannot be identified. As a consequence, the comparison of proteomic data sets between species will not identify every pair of homologous proteins whose abundances vary; instead, our goal is to understand differences in metabolism and cytoskeletal composition between species, based on changes in abundance of as many identified proteins as possible.

Warm acclimation

Despite the apparent differences in physiological responses to higher temperatures described above, *M. trossulus* and *M. galloprovincialis* do share similarities in their proteomic response to chronic heat exposure. For example, in each species, a comparable cluster of proteins is upregulated at 19°C (cluster 2; Figs 2, 3). Tubulin isoforms, which are important components of this cluster, form microtubules that are the basic structural elements of cilia that in *Mytilus* drive water flow through the gills. This active movement of water is necessary for respiration as well as for transporting mucus containing trapped food particles over the epithelium and along the ventral groove towards the mouth. Both acute and chronic exposure to warmer temperatures in *Mytilus* increase the filtration rate and particle transport (i.e. velocity along the ventral grove) without signs of temperature compensation (Kittner and Riisgård, 2005; Rao, 1953; Richoux and Thompson, 2001), and thus may require synthesis or remodeling of cilia. The increase in filtration rate at higher temperatures also likely requires higher rates of ATP production, which may be achieved by increasing the abundance of enzymes of the ETC and oxidative phosphorylation (Aiello, 1960; Malanga and Aiello, 1972). These include ubiquinol cytochrome *c* reductase (complex III of the ETC), succinate dehydrogenase (complex II, as well as a component of the Krebs cycle) and ATP synthase β-subunit, which are upregulated at 19°C in one or both species (Figs 2, 3, Table 1A). Note, however, that NADH dehydrogenase (complex I of the ETC) and pyruvate dehydrogenase (linking glycolysis to the Krebs cycle) are not part of this cluster in *M. galloprovincialis* but instead are upregulated at 13°C and downregulated at 19°C (Fig. 3; see below for further discussion).

Notably, cluster 2 also includes two classes of proteins unique to *M. trossulus* – molecular chaperones and oxidative stress proteins. In *M. trossulus* only, acclimation to 19°C increased levels or shifted the position, possibly due to PTMs, of several molecular chaperones: Hsp70, Hsp25 and an isoform of glucose-regulated protein 78 [Grp78, also known as binding immunoglobulin protein (BiP), is the Hsp70 homolog of the endoplasmic reticulum] (Fig. 2). The high component loadings for two of these proteins along PC1 (Table 1A,B) indicate that changes in their expression are an important part of the acclimation response to 19°C in *M. trossulus*. In addition to heat stress, the increased abundance of one DyP-type peroxidase isoform (another one is upregulated at 7 and 13°C), an enzyme that functions similarly to catalase and catalyzes the degradation of H_2O_2 to H_2O (Sugano, 2009), may suggest higher levels of oxidative stress at 19°C in *M. trossulus* but not in *M. galloprovincialis*.

Several studies have quantified changes in Hsp abundance and synthesis in response to high temperature in *Mytilus*. Anestis and colleagues (Anestis et al., 2007) showed that Hsp70 levels in *M. galloprovincialis* increase following acclimation to 26°C, whereas during seasonal acclimatization increases in abundance seem to occur at lower temperatures, perhaps just above 20°C (Hamer et al., 2004; Ioannou et al., 2009; Minier et al., 2000). Buckley et al. (Buckley et al., 2001) examined acclimation and acclimatization in *M. trossulus*, and found a difference in Hsp70 induction temperature depending on season (23°C in mussels collected in winter, 28°C in summer). In the single proteomics study comparing acute heat stress in both congeners, *M. trossulus* induced one Hsp70 isoform at 24°C, and *M. galloprovincialis* induced a heat shock cognate 70 isoform at 24°C, but interspecific differences in patterns of chaperone expression were complex at higher temperatures (Tomanek and Zuzow, 2010). In summary, it does not seem surprising that *M. galloprovincialis* shows no increase in Hsp abundance during acclimation to 19°C. The fact that *M. trossulus* changed the abundances (or positions) of several Hsps at the same temperature suggests that it regulates its chaperone activity in response to acclimation at this temperature. If position shifts within the 2-D gels indeed are underlying the ‘up-and-down’ pattern of several chaperones during acclimation (Fig. 2), it will be important to determine whether and which PTMs are causing these shifts and how they might change protein activity.

Cold acclimation

Protein cluster 1 (Figs 2, 3) is characterized by the upregulation of proteins at 7 and 13°C relative to the acclimation to 19°C. In both species, the proteins of this cluster fall into three functional categories: cytoskeletal proteins, molecular chaperones and oxidative stress proteins. Compared with the warm-acclimation cluster 2, cold acclimation leads to an increase in protein isoforms involved in chaperone activity and oxidative stress and a decrease in many cytoskeletal protein isoforms.

Among those cytoskeletal proteins that changed expression levels, we found mainly actin and tubulin isoforms, as we did in cluster 2, but fewer of them. Some of the changing levels of tubulin and actin isoforms may be related to changes of T-complex protein-1 (also known as chaperonin containing TCP-1 or CCT) and radial spoke head 9 (Figs 2, 3). The mature conformation of both actin and tubulin requires the folding cage of TCP-1 (Sternlicht et al., 1993), a key chaperone that also plays a role in the regulation of the formation of mitotic spindles and thus cell proliferation (Brackley and Grantham, 2009). In *M. galloprovincialis* only, T-complex protein-1 was upregulated at 7 and 13°C relative to 19°C (Fig. 3,

Table 1B), indicating that higher rates of folding of cytsokeletal proteins, possibly for the repair or generation of cilia, were required at these two temperatures in this warm-adapted species. Similarly, radial spoke head proteins are important components of the axoneme that forms the core of cilia. Radial spoke head 9 is upregulated in cluster 1 of both *M. galloprovincialis* and *M. trossulus*, suggesting increased synthesis or turnover of cilia at lower temperatures.

A second functional category present in cluster 1 includes molecular chaperones that are folding catalysts but are also involved in stabilizing proteins during unfolding due to proteotoxic stress (Hartl and Hayer-Hartl, 2002). In cold-acclimated *M. trossulus*, two isoforms of the major cellular chaperones Hsp70 and small Hsp (Hsp25) are upregulated (Fig. 2, Table 1B), with the latter playing an important role in stabilizing cytoskeletal elements during stress (Haslbeck et al., 2005). In addition, one isoform of Grp78 is upregulated (another, spot 79, is downregulated); the endoplasmic Grp78 is implicated, among other roles, in moderating the effects of oxidative stress (Liu et al., 1997). In *M. galloprovincialis*, the small Hsp21 shows upregulation in response to cold acclimation (Fig. 3), as does the β-subunit of prolyl 4-hydroxylase. Prolyl 4-hydroxylase holozyme modifies prolyl residues of collagens and several transcription factors, including hypoxia-inducible factor 1 (Gorres and Raines, 2010). Interestingly, though, the β-subunit of this heterotetramer is a protein disulfide isomerase (Koivunen et al., 2005; Vranka et al., 2004), whose role is to assist in the folding of proteins through the formation of disulfide bonds in the endoplasmic reticulum (Malhotra and Kaufman, 2007).

The third functional category in cluster 1 includes proteins involved in scavenging reactive oxygen species (ROS). For example, isoforms of NADP-dependent isocitrate dehydrogenase are upregulated during cold acclimation in both species. NADP-dependent IDH, an enzyme linked to the Krebs cycle, increases the [NADPH]/[NADP] ratio in the mitochondrion; the repair of macromolecules that suffer oxidative damage is dependent on high [NADPH], which is used to re-reduce glutathione (Jo et al., 2001). NADP-dependent IDH also has been hypothesized to play a role in the antioxidant response of *Mytilus* during acute heat stress (Tomanek and Zuzow, 2010).

Some oxidative stress proteins upregulated after cold acclimation are unique to each of the congeners. Examples in *M. galloprovincialis* include thioredoxin peroxidase (also known as peroxiredoxin), which detoxifies hydrogen peroxide or organic peroxides (Cox et al., 2010), and carbonyl reductase, which metabolizes lipid peroxidation products like carbonyl-containing aldehydes (Ellis, 2007). The function of selenium binding protein-1 is not known, but it may interact with glutathione peroxidase and thus affect the scavenging of ROS indirectly (Fang et al., 2010). In *M. trossulus*, DyP-type peroxidase catalyzes the conversion of H_2O_2 into H_2O (Sugano, 2009).

By reacting with unsaturated fatty acids, ROS produce many types of aldehydes, among the most common being malondialdehyde, hexanal and 4-hydroxynonenal (Ellis, 2007). Notably, according to the concept of homeoviscous adaptation, the levels of unsaturated phospholipids in membranes increase during cold acclimation to maintain membrane fluidity (Hazel and Williams, 1990). Thus it is likely that the level of cytotoxic aldehydes will increase as temperature decreases. In turn, these aldehydes cause protein carbonylation, which affects protein conformation and function, leading to protein denaturation (McDonagh et al., 2005). Based on these changes, an important oxidative stress protein upregulated during cold acclimation in both species is an isoform of aldehyde dehydrogenase (ALDH2) located in the mitochondrion (Ellis, 2007). In *M. galloprovincialis*, ALDH2 is upregulated at 13°C (Fig. 3), but its positive loading on PC2 (Table 1C) indicates that its abundance increases even further from 13 to 7°C. In contrast, in *M. trossulus*, ALDH2 has a highly negative loading for PC1 but not PC2 (Table 1B), indicating that it is upregulated at 13°C relative to 19°C, but does not increase significantly in abundance as temperature decreases further to 7°C.

Our results agree with those of other studies examining evidence for an increasing rate of oxidative stress, including lipid peroxidation, during cold acclimation in ectotherms. For example, proteomic changes similar to those described here were shown in a study on the response to cold stress of livers of warm-adapted gilthead sea bream (Ibarz et al., 2010); a study on cultivation temperatures of wild-type *C. elegans* larvae also showed increasing levels of chaperones and IDH in response to cold (Madi et al., 2003).

In addition to the differences between the species in clusters 1 and 2, the presence of clusters 3 and 4 in *M. galloprovincialis* (Fig. 3) provides further evidence that the proteomic responses to acclimation to 7 and 13°C differ between the congeners. Tubulin isoforms are the most abundant protein in the clusters unique to *M. galloprovincialis*. They, together with ATP-synthase β-subunit, contributed the most to the negative loadings of PC2, i.e. those indicating upregulation at 13°C relative to 7°C (Table 1D; see also Fig. 3). One potential explanation for this proliferation of tubulin isoforms could lay in the upregulation of formylglutathione hydrolase at 13°C, an enzyme that produces glutathione. Protein glutathionylation is an important and widespread reaction to protect sulfhydryl groups (Dalle-Donne et al., 2009), specifically in tubulins (Landino et al., 2004).

Chronic *versus* acute heat stress

Comparing the results of the present study with those of our previous analysis of proteomic changes during acute heat stress in the two *Mytilus* congeners (Tomanek and Zuzow, 2010) may offer insights into biochemical processes that are differently regulated between chronic and acute heat stress. For example, given that changes in tubulin can occur in clusters in which few or no concomitant changes in molecular chaperones are observed (13 and 19°C acclimation in *M. galloprovincialis*), changes in tubulin expression may not indicate thermal damage to the cytoskeletal network. Instead, changes in tubulin expression may correspond to changes in the activity of cilia due to increasing ventilation and filtration rates with increasing temperature (Kittner and Riisgård, 2005; Rao, 1953; Richoux and Thompson, 2001), or changing requirements for microtubules during cell proliferation. In contrast, during recovery from acute stress, changes in tubulin isoform expression occur in parallel with changes in chaperone abundance, especially in *M. galloprovincialis* (Tomanek and Zuzow, 2010).

In *M. trossulus*, we observed changes in a chaperone from the endoplasmic reticulum, Grp78, which did not change during acute heat stress (Tomanek and Zuzow, 2010). The total abundance of the two Grp78 isoforms (spots 76 and 79; data not shown) was greatest at 7 and 19°C, indicating that the endoplasmic reticulum of gill cells responds to both low and high temperature acclimation, but not to acute heat stress, with higher chaperoning capacity.

One pattern that appears to be common to both acute and chronic heat stress may represent a trade-off between the expression of oxidative stress proteins and proteins involved in energy metabolism. For example, during acclimation, both species show an upregulation of ubiquinol cytochrome *c* reductase (complex III of the ETC) at 19°C only. Complex III is a major site of ROS production (Andreyev

et al., 2005), but oxidative stress proteins increase in abundance mostly at 7 and 13°C (Figs 2, 3; DyP-type peroxidase in *M. trossulus* being the only exception). At least in *M. galloprovincialis*, protein expression patterns may also indicate additional adjustments in energy metabolism, e.g. upregulation of succinate dehydrogenase and downregulation of NADH dehydrogenase at 19°C, downregulation of pyruvate dehydrogenase at 19°C, and upregulation of ATP-synthase β subunit isoforms at 13°C (spot 59) and 19°C (spot 143). These changes did not occur in *M. galloprovincialis* during acute heat stress and could indicate that chronic adjustments, due to cold-induced oxidative stress *versus* a heat-induced increase in ventilation rate, force different trade-offs between limiting oxidative stress and maintaining an appropriate level of ATP production.

Similarly, the NADP-dependent IDH isoforms we detected are part of the Krebs cycle and play an important regulatory role in maintaining a constant ratio of reduced to oxidized glutathione, which in turn controls the antioxidant potential of the cell (Jo et al., 2001). IDH isoforms changed abundances during acute heat stress in *M. trossulus*, consistent with an increasing role in scavenging ROS (Tomanek and Zuzow, 2010). Here, all IDH isoforms (spot 75 in *M. galloprovincialis*; spots 68 and 73 in *M. trossulus*) have high positive loadings for PC2 and are more abundant at 7°C relative to 13°C (although two of these isoforms, spots 75 in *M. galloprovincialis* and 68 in *M. trossulus*, are also more abundant at 19°C compared with 13°C, their PC1 loadings are negligible). In contrast to mitochondrial IDH expression, several enzymes of the cytosolic pentose phosphate pathway that provide reducing equivalents in form of NADPH during acute heat stress did not change during chronic temperature stress in either congener.

Overall, a broad comparison of the proteomic data sets derived from chronic and acute temperature stress suggests that oxidative stress levels seem to be high in chronically cold-acclimated as well as acutely heat-stressed mussels. Thus, the combination of cold acclimation (or acclimatization) followed by acute heat exposure could represent a particularly severe level of stress and be a major limiting factor in setting distribution ranges, a notion that is now supported by a number of physiological data sets (Tomanek, 2008; Tomanek, 2010).

In summary, both congeners experience cold-induced oxidative stress, with the relatively warm-adapted *M. galloprovincialis* showing different expression patterns between 7 and 13°C (possibly because of tubulin isoform expression) whereas the cold-adapted *M. trossulus* responds with a single expression pattern to both temperatures. Cold-induced oxidative stress also may cause re-arrangements in energy metabolism in both species, e.g. downregulation of ubiquinol cytochrome *c* reductase and ATP synthase, again with different expression patterns between 7 and 13°C in *M. galloprovincialis* only. At the warmest acclimation temperature, both species show an upregulation of several tubulin isoforms and ubiquinol cytochrome *c* reductase, in agreement with previous studies that showed that filtration and respiration rates increase with increasing temperature due to enhanced ciliary activity (Aiello, 1960; Gray, 1924). Furthermore, during acclimation to 19°C, *M. trossulus*, but not *M. galloprovincialis*, shows increasing abundances of molecular chaperones, suggesting that this temperature is close to its chronic thermal limit.

LIST OF ABBREVIATIONS

2DGE	two-dimensional gel electrophoresis
ADP (ATP)	adenosine di-(tri)-phosphate
ALDH	aldehyde dehydrogenase
EST	expressed sequence tag
ETC	electron transport chain
Grp78	glucose-regulated protein 78
Hsp	heat shock protein
IDH	isocitrate dehydrogenase
IPG	immobilized pH gradient
MALDI-TOF-TOF	matrix-assisted laser desorption ionization tandem time-of-flight
MOWSE	molecular weight search
MS/MS	tandem mass spectrometry
NAD(H)	nicotinamide adenine dinucleotide (reduced form)
NADP(H)	nicotinamide adenine dinucleotide phosphate (reduced form)
PC	principal component
PCA	principal component analysis
PMF	peptide mass fingerprint
PTM	post-translational modification
ROS	reactive oxygen species
TCP-1	T-complex protein 1
TFA	trifluoroacetic acid

FUNDING

This work was supported by the National Science Foundation [grants IOS-0717087 to L.T. and IOS-0920103 to P.A.F.].

REFERENCES

Aiello, E. L. (1960). Factors affecting ciliary activity on the gill of the mussel *Mytilus edulis*. *Physiol. Zool.* **33**, 120-135.
Andreyev, A. Y., Kushnareva, Y. E. and Starkov, A. A. (2005). Mitochondrial metabolism of reactive oxygen species. *Biochemistry* **70**, 200-214.
Anestis, A., Lazou, A., Portner, H. O. and Michaelidis, B. (2007). Behavioral, metabolic, and molecular stress responses of marine bivalve *Mytilus galloprovincialis* during long-term acclimation at increasing ambient temperature. *Am. J. Physiol. Regul. Integr. Comp. Physiol.* **293**, R911-R921.
Apraiz, I., Mi, J. and Cristobal, S. (2006). Identification of proteomic signatures of exposure to marine pollutants in mussels (*Mytilus edulis*). *Mol. Cell Proteomics* **5**, 1274-1285.
Barry, J. P., Baxter, C. H., Sagarin, R. D. and Gilman, S. E. (1995). Climate-related, long-term faunal changes in a California rocky intertidal community. *Science* **267**, 672-675.
Berth, M., Moser, F. M., Kolbe, M. and Bernhardt, J. (2007). The state of the art in the analysis of two-dimensional gel electrophoresis images. *Appl. Microbiol. Biotechnol.* **76**, 1223-1243.
Braby, C. E. and Somero, G. N. (2006). Following the heart: temperature and salinity effects on heart rate in native and invasive species of the blue mussels (genus *Mytilus*). *J. Exp. Biol.* **209**, 2554-2566.
Brackley, K. I. and Grantham, J. (2009). Activities of the chaperonin containing TCP-1 (CCT): implications for cell cycle progression and cytoskeletal organisation. *Cell Stress Chaperones* **14**, 23-31.
Buckley, B. A., Owen, M.-E. and Hofmann, G. E. (2001). Adjusting the thermostat: the threshold induction temperature for the heat-shock response in intertidal mussels (genus *Mytilus*) changes as a function of thermal history. *J. Exp. Biol.* **204**, 2816-2829.
Cox, A. G., Winterbourn, C. C. and Hampton, M. B. (2010). Mitochondrial peroxiredoxin involvement in antioxidant defence and redox signaling. *Biochem. J.* **425**, 313-325.
Dalle-Donne, I., Rossi, R., Colombo, G., Giustarini, D. and Milzani, A. (2009). Protein S-glutathionylation: a regulatory device from bacteria to humans. *Trends Biochem. Sci.* **34**, 85-96.
Ellis, E. M. (2007). Reactive carbonyls and oxidative stress: potential for therapeutic intervention. *Pharmacol. Ther.* **115**, 13-24.
Evans, T. G. and Somero, G. N. (2010). Phosphorylation events catalyzed by major cell signaling proteins differ in response to thermal and osmotic stress among native (*Mytilus californianus* and *Mytilus trossulus*) and invasive (*Mytilus galloprovincialis*) species of mussels. *Physiol. Biochem. Zool.* **83**, 984-996.
Fang, W., Goldberg, M. L., Pohl, N. M., Bi, X., Tong, C., Xiong, B., Koh, T. J., Diamond, A. M. and Yang, W. (2010). Functional and physical interaction between the selenium-binding protein 1 (SBP1) and the glutathione peroxidase 1 selenoprotein. *Carcinogenesis* **31**, 1360-1366.
Fields, P. A., Rudomin, E. L. and Somero, G. N. (2006). Temperature sensitivities of cytosolic malate dehydrogenases from native and invasive species of marine mussels (genus *Mytilus*): sequence-function linkages and correlations with biogeographic distribution. *J. Exp. Biol.* **209**, 656-667.
Geller, J. B. (1999). Decline of a native mussel masked by sibling species invasion. *Conserv. Biol.* **13**, 661-664.
Gorres, K. L. and Raines, R. T. (2010). Prolyl 4-hydroxylase. *Crit. Rev. Biochem. Mol. Biol.* **45**, 106-124.
Gray, J. (1924). The mechanism of ciliary movement – IV. The relation of ciliary activity to oxygen consumption. *Proc. R. Soc. Lond. B* **96**, 95-114.
Hamer, B., Hamer, D. P., Muller, W. E. and Batel, R. (2004). Stress-70 proteins in marine mussel *Mytilus galloprovincialis* as biomarkers of environmental pollution: a field study. *Environ. Int.* **30**, 873-882.
Hansen, J., Sato, M., Ruedy, R., Lo, K., Lea, D. W. and Medina-Elizade, M. (2006). Global temperature change. *Proc. Natl. Acad. Sci. USA* **103**, 14288-14293.

Hartl, F. U. and Hayer-Hartl, M. (2002). Molecular chaperones in the cytosol: from nascent chain to folded protein. *Science* **295**, 1852-1858.
Haslbeck, M., Franzmann, T., Weinfurtner, D. and Buchner, J. (2005). Some like it hot: the structure and function of small heat-shock proteins. *Nat. Struct. Mol. Biol.* **12**, 842-846.
Hazel, J. R. and Williams, E. E. (1990). The role of alterations in membrane lipid composition in enabling physiological adaptation of organisms to their physical environment. *Prog. Lipid Res.* **29**, 167-227.
Hilbish, T. J., Brannock, P. M., Jones, K. R., Smith, A. B., Bullock, B. N. and Wethey, D. S. (2010). Historical changes in the distributions of invasive and endemic marine invertebrates are contrary to global warming predictions: the effects of decadal climate oscillations. *J. Biogeogr.* **37**, 423-431.
Hochachka, P. W. and Somero, G. N. (2002). *Biochemical Adaptation: Mechanism and Process in Physiological Evolution.* Oxford: Oxford University Press.
Hofmann, G. E. and Somero, G. N. (1996). Interspecific variation in thermal denaturation of proteins in the congeneric mussels *Mytilus trossulus* and *M. galloprovincialis*: evidence from the heat-shock response and protein ubiquitination. *Mar. Biol.* **126**, 65-75.
Ibarz, A., Martin-Perez, M., Blasco, J., Bellido, D., de Oliveira, E. and Fernandez-Borras, J. (2010). Gilthead sea bream liver proteome altered at low temperatures by oxidative stress. *Proteomics* **10**, 963-975.
Ioannou, S., Anestis, A., Pörtner, H. O. and Michaelidis, B. (2009). Seasonal patterns of metabolism and the heat shock response (HSR) in farmed mussels *Mytilus galloprovincialis*. *J. Exp. Mar. Biol. Ecol.* **381**, 136-144.
Jo, S. H., Son, M. K., Koh, H. J., Lee, S. M., Song, I. H., Kim, Y. O., Lee, Y. S., Jeong, K. S., Kim, W. B., Park, J. W. et al. (2001). Control of mitochondrial redox balance and cellular defense against oxidative damage by mitochondrial NADP+-dependent isocitrate dehydrogenase. *J. Biol. Chem.* **276**, 16168-16176.
Jones, S. J., Mieszkowska, N. and Wethey, D. S. (2009). Linking thermal tolerances and biogeography: *Mytilus edulis* (L.) at its southern limit on the east coast of the United States. *Biol. Bull.* **217**, 73-85.
Kittner, C. and Riisgård, H. U. (2005). Effect of temperature on filtration rate in the mussel *Mytilus edulis*: no evidence for temperature compensation. *Mar. Ecol. Prog. Ser.* **305**, 147-152.
Koivunen, P., Salo, K. E. H., Myllyharju, J. and Ruddock, L. W. (2005). Three binding sites in protein-disulfide isomerase cooperate in collagen prolyl 4-hydroxylase tetramer assembly. *J. Biol. Chem.* **280**, 5227-5235.
Landino, L. M., Moynihan, K. L., Todd, J. V. and Kennett, K. L. (2004). Modulation of the redox state of tubulin by the glutathione/glutaredoxin reductase system. *Biochem. Biophys. Res. Commun.* **314**, 555-560.
Liu, H., Bowes, R. C., III, van de Water, B., Sillence, C., Nagelkerke, J. F. and Stevens, J. L. (1997). Endoplasmic reticulum chaperones GRP78 and calreticulin prevent oxidative stress, Ca2+ disturbances, and cell death in renal epithelial cells. *J. Biol. Chem.* **272**, 21751-9.
Lockwood, B. L., Sanders, J. G. and Somero, G. N. (2010). Transcriptomic responses to heat stress in invasive and native blue mussels (genus *Mytilus*): molecular correlates of invasive success. *J. Exp. Biol.* **213**, 3548-3558.
Lovrić, J. (2010). *Introducing Proteomics: From Concepts to Sample Preparation, Mass Spectrometry and Data Analysis.* Oxford: Wiley-Blackwell.
Madi, A., Mikkat, S., Ringel, B., Ulbrich, M., Thiesen, H. J. and Glocker, M. O. (2003). Mass spectrometric proteome analysis for profiling temperature-dependent changes of protein expression in wild-type Caenorhabditis elegans. *Proteomics* **3**, 1526-1534.
Malanga, C. J. and Aiello, E. L. (1972). Succinate metabolismin the gills of the mussels *Modiolus demissus* and *Mytilus edulis*. *Comp. Biochem. Physiol.* **43B**, 795-806.
Malhotra, J. D. and Kaufman, R. J. (2007). The endoplasmic reticulum and the unfolded protein response. *Semin. Cell Dev. Biol.* **18**, 716-731.
McDonagh, B. and Sheehan, D. (2007). Effect of oxidative stress on protein thiols in the blue mussel Mytilus edulis: proteomic identification of target proteins. *Proteomics* **7**, 3395-3403.
McDonagh, B., Tyther, R. and Sheehan, D. (2005). Carbonylation and glutathionylation of proteins in the blue mussel *Mytilus edulis* detected by proteomic analysis and Western blotting: actin as a target for oxidative stress. *Aquat. Toxicol.* **73**, 315-326.
Mieszkowska, N., Kendall, M. A., Hawkins, S. J., Leaper, R., Williamson, P., Hardman-Mountford, N. J. and Southward, A. J. (2006). Changes in the range of some common rocky shore species in Britain – a response to climate change? *Hydrobiologia* **555**, 241-251.
Minier, C., Borghi, V. V., Moore, M. N. and Porte, C. (2000). Seasonal variation of MXR and stress proteins in the common mussel, *Mytilus galloprovincialis*. *Aquat. Toxicol.* **50**, 167-176.
Parmesan, C., Ryrholm, N., Stefanescus, C., Hill, J. K., Thomas, C. D., Descimon, H., Huntley, B., Kaila, L., Kullberg, J., Tammaru, T. et al. (1999). Poleward shifts in geographical ranges of butterfly species associated with regional warming. *Nature* **399**, 579-584.
Pörtner, H.-O. (2010). Oxygen- and capacity-limitation of thermal tolerance: a matrix for integrating climate-related stressor effects in marine ecosystems. *J. Exp. Biol.* **213**, 881-893.
Rao, K. P. (1953). Rate of water propulsion in *Mytilus californianus* as function of latititude. *Biol. Bull.* **104**, 171-181.
Richoux, N. B. and Thompson, R. J. (2001). Regulation of particle transport within the ventral groove of the mussel (*Mytilus edulis*) gill in response to environmental conditions. *J. Exp. Mar. Biol. Ecol.* **260**, 199-215.
Sarver, S. K. and Foltz, D. W. (1993). Genetic population structure of a species complex of blue mussels (*Mytilus* spp.). *Mar. Biol.* **117**, 105-112.
Schneider, K. R. (2008). Heat stress in the intertidal: comparing survival and growth of an invasive and native mussel under a variety of thermal conditions. *Biol. Bull.* **215**, 253-264.
Schneider, K. R. and Helmuth, B. (2007). Spatial variability in habitat temperature may drive patterns of selection between an invasive and native mussel species. *Mar. Ecol. Prog. Ser.* **339**, 157-167.
Serafini, L., Hann, J. B., Kültz, D. and Tomanek, L. (2011). The proteomic response of sea squirts (genus *Ciona*) to acute heat stress: a global perspective on the thermal stability of proteins. *Comp. Biochem. Physiol.* **6D**, 322-334.
Sheehan, D. (2007). The potential of proteomics for providing new insights into environmental impacts on human health. *Rev. Environ. Health* **22**, 175-194.
Sternlicht, H., Farr, G. W., Sternlicht, M. L., Driscoll, J. K., Willison, K. and Yaffe, M. B. (1993). The t-complex polypeptide 1 complex is a chaperonin for tubulin and actin in vivo. *Proc. Natl. Acad. Sci. USA* **90**, 9422-9426.
Sugano, Y. (2009). DyP-type peroxidases comprise a novel heme peroxidase family. *Cell. Mol. Life Sci.* **66**, 1387-1403.
Thomas, C. D. and Lennon, J. J. (1999). Birds extend their ranges northwards. *Nature* **399**, 213.
Tomanek, L. (2008). The importance of physiological limits in determining biogeographical range shifts due to global climate change: the heat-shock response. *Physiol. Biochem. Zool.* **81**, 709-717.
Tomanek, L. (2010). Variation in the heat shock response and its implication for predicting the effect of global climate change on species' bioegographic distribution ranges and metabolic costs. *J. Exp. Biol.* **213**, 971-979.
Tomanek, L. (2011). Environmental proteomics: changes in the proteome of marine organisms in response to environmental stress, pollutants, infection, symbiosis and development. *Annu. Rev. Mar. Sci.* **3**, 373-399.
Tomanek, L. and Zuzow, M. J. (2010). The proteomic response of the mussel congeners *Mytilus galloprovincialis* and *M. trossulus* to acute heat stress: implications for thermal tolerance and metabolic costs of thermal stress. *J. Exp. Biol.* **213**, 3559-3574.
Tomanek, L., Zuzow, M. J., Ivanina, A. V., Beniash, E. and Sokolova, I. M. (2011). Proteomic response to elevated P_{CO2} level in eastern oysters *Crassostrea virginica*: evidence for oxidative stress. *J. Exp. Biol.* **214**, 1836-1844.
Vranka, J. A., Sakai, L. Y. and Bächinger, H. P. (2004). Prolyl 3-hydroxylase 1, enzyme characterization and identification of a novel family of enzymes. *J. Biol. Chem.* **279**, 23615-23621.
Walsh, C. T., Garneau-Tsodikova, S. and Gatto, G. J. (2005). Protein posttranslational modifications: the chemistry of proteome diversifications. *Angew. Chem. Int. Ed.* **44**, 7342-7372.
Wonham, M. J. (2004). Distribution of the Mediterranean mussel *Mytilus galloprovincialis* (Bivalvia: Mytilidae) and hybrids in the Northeast Pacific. *J. Shellfish Res.* **23**, 535-543.

Table S1. Protein identifications (using MS/MS) of spots changing with temperature acclimation in *Mytilus trossulus*

Spot ID	Protein ID	Estimated molecular weight (kDa)	Estimated pI	Predicted molecular weight (kDa)	Predicted pI	GenBank ID	Mascot score	Peptide matches	Sequence coverage(%)	Average volume (relative to 13°C) 7°C	19°C	Functional category
2	Hsp70	70	5.73	70	5.30	gil145885532	273	3	16	0.84	3.39	Molecular chaperone
5	mitochondrial Aldehyde dehydrogenase	57	5.59	56	6.70	gil58307245	89	2	9	1.16	0.29	Proteolysis/energy metabolism
8	Ubiquinol cytochrome *c* reductase	49	5.72	48	5.93	gil223027244	182	4	23	0.54	2.46	Energy metabolism
12	β-Tubulin	53	5.12	43	5.76	gil164592164	228	5	17	0.95	1.66	Cytoskeletal
13	β-Tubulin	54	5.13	43	5.76	gil164592164	314	8	25	0.94	1.80	Cytoskeletal
14	β-Tubulin	50	5.00	43	5.76	gil164592164	304	7	22	0.89	2.35	Cytoskeletal
15	α-Tubulin	67	5.18	58	4.90	gil238782438	486	7	27	1.37	2.48	Cytoskeletal
16	α-Tubulin	66	5.24	58	4.90	gil238782438	404	5	19	0.90	2.86	Cytoskeletal
17	β-Tubulin	53	4.95	43	5.76	gil164592164	196	4	17	0.55	1.38	Cytoskeletal
18	Hsp25	57	5.69	22	6.52	gil212814271	115	2	9	1.08	0.45	Molecular chaperone
24	β-Tubulin	51	5.59	54	4.92	gil145890511	181	4	12	1.39	5.39	Cytoskeletal
25	Ubiquinol cytochrome *c* reductase	50	5.4	48	9.00	gil212817136	68	2	4	1.14	2.91	Proteolysis/energy metabolism
27	Heavy metal binding protein	37	5.31	27	5.00	gil58308171	152	2	13	0.68	0.65	Unspecified
28	Hsp25	31	5.26	22	6.52	gil212814271	108	2	9	0.53	0.49	Molecular chaperone
32	Dyp-type peroxidase	35	6.48	42	7.00	gil145886780	95	3	12	0.59	2.56	Energy metabolism
36	Quinoid dihydropteridine reductase	31	6.62	25	6.58	gil212827262	116	3	10	0.88	0.25	Energy metabolism
37	Dyp-type peroxidase	33	6.49	42	7.00	gil145886780	111	3	12	1.06	0.30	Energy metabolism
40	Hsp25	33	6.31	22	6.52	gil212814271	82	2	9	1.08	2.82	Molecular chaperone
43	Hsc71	76	5.33	71	5.29	gil212816159	79	5	16	1.12	0.40	Molecular chaperone
45	Gelsolin	49	6.16	42	5.22	gil149382505	228	3	17	1.69	8.44	Cytoskeletal
52	Hsp70	60	5.98	70	5.30	gil145885532	170	2	10	1.10	0.26	Molecular chaperone
54	Tektin-3	53	5.9	57	7.22	gil212812350	98	2	13	1.04	0.53	Cytoskeletal
55	Ubiquinol cytochrome *c* reductase	47	5.81	48	5.93	gil223027244	182	4	23	0.60	1.86	Proteolysis/energy metabolism
58	Ubiquinol cytochrome *c* reductase	49	5.95	48	5.93	gil223027244	89	2	13	1.20	3.46	Proteolysis/energy metabolism
59	β-Actin	49	5.88	39	5.80	gil49868	92	2	7	0.57	3.06	Cytoskeletal

60	Radial spoke head 9	38	6.07	31	4.97	gil223025866	78	2	9	0.78	0.38	Unspecified
61	β-Actin	50	5.82	39	5.80	gil49868	154	4	15	0.81	0.37	Cytoskeletal
67	α-Tubulin	47	5.41	58	4.90	gil238782438	404	5	19	1.59	0.56	Cytoskeletal
68	Isocitrate dehydrogenase (NADP)	45	6.61	51	7.91	gil223026036	178	4	18	1.41	1.30	Energy metabolism
73	Isocitrate dehydrogenase (NADP)	44	6.49	51	7.91	gil223026036	77	3	13	1.79	1.14	Energy metabolism
76	78kD glucose regulated protein	88	6.48	73	5.00	gil46359618	73	2	3	2.44	0.88	Unspecified
78	β-Tubulin	57	4.79	43	5.69	gil58307872	151	5	23	1.10	0.37	Cytoskeletal
79	78kD glucose regulated protein	89	4.85	73	5.00	gil238639954	245	4	24	0.88	2.53	Unspecified

pI, isoelectric point.

Table S2. Protein identifications (using MS/MS) of spots changing with temperature acclimation in *Mytilus galloprovincialis*

Spot ID	Protein ID	Estimated molecular weight (kDa)	Estimated pI	Predicted molecular weight (kDa)	Predicted pI	GenBank ID	Mascot score	Peptide matches	Sequence coverage (%)	Average volume (relative to 13°C) 7°C	Average volume (relative to 13°C) 19°C	Functional category
2	Prohibitin	30	5.43	30	5.30	gil238643256	211	5	17	0.99	0.25	Molecular chaperone
4	Carbonyl reductase	31	5.18	30	8.50	gil145883693	59	2	8	0.75	0.28	Energy metabolism
9	NADH dehydrogenase	28	4.75	24	5.74	gil223028674	43	2	14	0.55	0.25	Energy metabolism
11	Actin	29	5.55	42	5.30	gil212814343	104	4	19	0.61	0.30	Cytoskeletal
12	Hsp21	34	5.52	21	6.70	gil238642855	107	3	16	0.48	0.22	Molecular chaperone
26	Succinate dehydrogenase (Ubiquinone)	66	5.89	72	6.70	gil18426858	80	3	5	0.39	4.08	Energy metabolism
30	α-Tubulin	56	5.08	57	5.00	gil145887917	233	5	18	0.45	0.64	Cytoskeletal
34	Selenium binding protein-1	55	5.78	54	6.50	gil58307672	51	2	11	1.09	0.57	Unspecified
37	α-Tubulin	53	4.94	58	4.90	gil238782438	260	6	25	0.37	0.38	Cytoskeletal
38	α-Tubulin	56	5	57	5.00	gil145887917	238	5	15	0.33	0.48	Cytoskeletal
39	α-Tubulin	56	4.98	57	5.00	gil145887917	159	5	15	0.47	0.16	Cytoskeletal
41	α-Tubulin	55	5.16	57	5.00	gil212817436	204	5	18	0.35	0.37	Cytoskeletal
44	α-Tubulin	55	5.03	53	5.00	gil58307555	89	2	13	0.30	0.19	Cytoskeletal
45	α-Tubulin	53	4.82	47	5.23	gil154349830	158	3	12	0.75	0.19	Cytoskeletal
46	β-Tubulin	53	4.85	43	5.76	gil164592164	180	6	17	0.44	0.04	Cytoskeletal
48	α-Tubulin	53	4.88	47	5.23	gil154349830	202	3	12	0.35	0.22	Cytoskeletal
52	β-Tubulin	53	4.73	54	4.92	gil145890511	95	4	8	0.73	0.29	Cytoskeletal
54	β-Tubulin	52	5.03	54	4.90	gil145890511	124	4	12	0.35	1.25	Cytoskeletal
55	Ubiquinol cytochrome *c* reductase	52	5.74	53	5.40	gil145883486	56	2	9	0.19	5.51	Energy metabolism
56	Tropomyosin	51	5.1	33	4.70	gil14285796	167	6	15	0.40	6.03	Cytoskeletal
58	Intermediate filament	51	5.16	71	5.40	gil212812257	53	3	16	0.42	6.61	Cytoskeletal
59	ATP synthase β-subunit	50	4.84	57	5.38	gil212812392	490	8	42	0.40	0.61	Energy metabolism
62	Mitochondrial aldehyde dehydrogenase	50	5.56	56	6.70	gil58307245	74	2	9	0.63	12.55	Energy metabolism
66	β-Tubulin	49	4.97	43	5.80	gil164592164	247	7	17	0.40	7.95	Cytoskeletal
75	Isocitrate dehydrogenase (NADP)	46	6.79	51	7.91	gil223026036	102	3	13	8.33	4.67	Energy metabolism
77	Actin	45	5.24	42	5.30	gil145892505	78	5	13	0.95	0.50	Cytoskeletal
78	Ubiquinol cytochrome *c* reductase	46	5.68	53	5.40	gil164595882	80	3	9	1.59	13.13	Energy metabolism
87	Actin	43	5.22	42	5.30	gil212827318	210	4	18	0.73	4.15	Cytoskeletal
88	Actin	43	5.27	42	5.30	gil212827318	166	4	18	0.66	3.52	Cytoskeletal
89	Actin	43	5.41	42	5.30	gil212827318	185	4	18	0.20	2.04	Cytoskeletal
93	α-Tubulin	39	5.39	58	4.90	gil238782438	261	7	29	0.71	5.44	Cytoskeletal
103	β-Tubulin	36	5.36	43	5.80	gil164592164	151	6	22	0.88	2.96	Cytoskeletal
106	Radial spoke head 9	36	5.98	31	4.97	gil223025866	250	6	29	1.49	0.49	Unspecified
113	Esterase D/formylglutathione	33	6.42	31	6.00	gil223022457	67	2	12	0.18	0.16	Energy metabolism

	hydrolase											
120	β-Tubulin	32	4.9	43	5.80	gil164592164	185	6	20	1.01	0.22	Cytoskeletal
123	Fibrinogen related domain	31	6.79	27	6.10	gil154349256	75	3	7	4.35	3.39	Cytoskeletal
124	Hsp21	31	5.85	21	6.70	gil238642855	226	4	28	1.25	0.14	Molecular chaperone
125	Proteasome α-type-4	32	6.26	30	6.90	gil164594998	65	2	9	2.17	1.22	Protein degradation
126	Cyclophilin 3	30	6.74	27	5.10	gil145882165	186	5	15	4.76	5.57	Cytoskeletal
128	Proteasome α-type-6	30	6.31	27	6.35	gil212811956	111	2	9	1.28	0.41	Protein degradation
132	T complex protein-1	29	6.2	53	5.46	gil212817064	54	2	9	1.19	0.04	Unspecified
133	Mitochondrial aldehyde dehydrogenase	28	6.48	56	6.69	gil58307245	58	2	9	1.35	0.26	Energy metabolism
135	Thioredoxin peroxidase	26	6.63	32	5.50	gil145895058	89	4	12	2.56	0.33	Energy metabolism
141	Prolyl 4-hydroxylase β-subunit precursor	56	4.55	57	4.80	gil212815598	73	2	9	0.84	0.44	Energy metabolism
143	ATP synthase β-subunit	48	4.83	57	5.40	gil212812392	306	7	32	0.85	4.44	Energy metabolism
144	Major Vault Protein	108	5.73	96	5.70	gil223026493	61	3	13	2.78	1.61	Unspecified
145	Pyruvate dehydrogenase	35	5.45	39	5.80	gil58307688	44	2	3	1.02	0.58	Energy metabolism
146	Actin	41	5.01	42	5.30	gil145892505	252	6	21	0.44	0.49	Cytoskeletal

pI, isoelectric point.